PLOS ONE

RESEARCH ARTICLE

Diversity and relative abundance of ammonia- and nitrite-oxidizing microorganisms in the offshore Namibian hypoxic zone

Evan Lau[1,2]*, Caitlin H. Frame[3], E. Joseph Nolan IV[2], Frank J. Stewart[4], Zachary W. Dillard[2], Daniel P. Lukich[2], Nicole E. Mihalik[2], Katelyn E. Yauch[2], Marcus A. Kinker[2], Samantha L. Waychoff[2]

1 Department of Biology, Menlo College, Atherton, California, United States of America, **2** Department of Natural Sciences and Mathematics, West Liberty University, West Liberty, West Virginia, United States of America, **3** Department of Environmental Sciences, University of Basel, Basel, Switzerland, **4** School of Biological Sciences, Georgia Institute of Technology, Atlanta, Georgia, United States of America

* evanlau28@gmail.com

OPEN ACCESS

Citation: Lau E, Frame CH, Nolan EJ IV, Stewart FJ, Dillard ZW, Lukich DP, et al. (2019) Diversity and relative abundance of ammonia- and nitrite-oxidizing microorganisms in the offshore Namibian hypoxic zone. PLoS ONE 14(5): e0217136. https://doi.org/10.1371/journal.pone.0217136

Editor: Hongbin Liu, Hong Kong University of Science and Technology, HONG KONG

Received: September 19, 2018

Accepted: May 6, 2019

Published: May 21, 2019

Copyright: © 2019 Lau et al. This is an open access article distributed under the terms of the Creative Commons Attribution License, which permits unrestricted use, distribution, and reproduction in any medium, provided the original author and source are credited.

Data Availability Statement: All relevant data are within the manuscript and its Supporting Information files.

Funding: EL received grants from National Institutes of Health West Virginia IDeA Network of Biomedical Research Excellence, WV-INBRE, award# 2P20GM103434-14, http://www.wv-inbre.net. EL received a grant from the West Liberty University Faculty Development Fund, https://westliberty.edu. CHF received a grant from Freiwillige Akademische Gesellschaft of Basel,

Abstract

Nitrification, the microbial oxidation of ammonia (NH_3) to nitrite (NO_2^-) and NO_2^- to nitrate (NO_3^-), plays a vital role in ocean nitrogen cycling. Characterizing the distribution of nitrifying organisms over environmental gradients can help predict how nitrogen availability may change with shifting ocean conditions, for example, due to loss of dissolved oxygen (O_2). We characterized the distribution of nitrifiers at 5 depths spanning the oxic to hypoxic zone of the offshore Benguela upwelling system above the continental slope off Namibia. Based on 16S rRNA gene amplicon sequencing, the proportional abundance of nitrifiers (ammonia and nitrite oxidizers) increased with depth, driven by an increase in ammonia-oxidizing archaea (AOA; Thaumarchaeota) to up to 33% of the community at hypoxic depths where O_2 concentrations fell to ~25 μM. The AOA community transitioned from being dominated by a few members at oxic depths to a more even representation of taxa in the hypoxic zone. In comparison, the community of NO_2^--oxidizing bacteria (NOB), composed primarily of Nitrospinae, was far less abundant and exhibited higher evenness at all depths. The AOA: NOB ratio declined with depth from 41:1 in the oxic zone to 27:1 under hypoxia, suggesting potential variation in the balance between NO_2^- production and consumption via nitrification. Indeed, in contrast to prior observations from more O_2-depleted sites closer to shore, NO_2^- did not accumulate at hypoxic depths near this offshore site, potentially due in part to a tightened coupling between AOA and NOB.

Introduction

Microbial nitrification plays an important role in regulating the availability of nitrogen (N) for biological consumption. In the first step of nitrification, ammonia (NH_3) is oxidized to nitrite (NO_2^-) by ammonia-oxidizing archaea (AOA) or bacteria (AOB), with AOA of the phylum Thaumarchaeota playing a major role in NH_3 oxidation in marine systems [1–3]. In the second

Switzerland, through University of Basel, https://www.sareco.org/institution/freiwillige-akademische-gesellschaft-basel-fag and Swiss National Science Foundation Grant NUW1530. The funders had no role in study design, data collection and analysis, decision to publish, or preparation of the manuscript.

Competing interests: The authors have declared that no competing interests exist.

nitrification step, NO_2^- is oxidized to nitrate (NO_3^-) by nitrite-oxidizing bacteria (NOB), with members of the *Nitrospina* (Nitrospinae), *Nitrococcus* (Gammaproteobacteria), and *Nitrospira* (Nitrospirae) among the most common NOB in marine systems [4–8]. The microbes mediating these two steps can be spatially separated or active at different times based on environmental conditions, including the concentrations of inorganic N substrates and dissolved O_2 [e.g., 9–11]. Alternatively, AOA/AOB and NOB activity can be tightly coupled, with no NO_2^- accumulation [e.g., 11,12]. Characterizing the distribution of nitrifying taxa in diverse habitats, such as sites with low dissolved O_2 concentrations, can help determine the physical or chemical thresholds that decouple NH_3 oxidation from NO_2^- oxidation, and therefore help predict the accumulation and flux of inorganic N in ocean systems.

Nitrifying microorganisms are abundant in and at the periphery of marine zones where dissolved O_2 concentrations decline, including the upwelling-driven oxygen minimum zones (OMZs) of the eastern Pacific [13,14] and the Benguela upwelling system off Namibia [7]. At the core of these zones, dissolved O_2 concentration is in the low nanomolar (nM) range [15,16]. Anaerobic metabolisms dominate under these conditions. Such metabolisms include both denitrification, which begins with the NO_2^--producing step of NO_3^- reduction, as well as anaerobic ammonia oxidation (anammox) with NO_2^-, a process that may compete with NOB for NO_2^-. These anaerobic processes, however, are substantially suppressed as dissolved O_2 rises to levels of just a few micromolar (μM), which are sufficient to concurrently enable a range of aerobic metabolisms [12,17]. Notably, in the transition zone from near-anoxia to hypoxia (a few to tens of μM O_2), low O_2-adapted nitrifiers make substantial contributions to N cycling [13,14,18,19]. In this zone, coupling between the two nitrification steps may be a primary control over the availability and accumulation of inorganic N intermediates that feed both oxidative and reductive metabolisms, including NO_2^- and the greenhouse gas nitrous oxide (N_2O) [11,13,20–22]. Thus, there is considerable interest in understanding nitrifier abundance, diversity, and activity as O_2 concentration declines [7,13,23].

The Benguela upwelling system is an ideal model for exploring nitrifier community structure over varying O_2 regimes. In this system, coastal upwelling of nutrient-rich water extends from the southern tip of Africa (~35˚S) to the Angola front (~15˚S), reaching peak magnitude off Namibia [24]. The resulting high levels of primary production drive O_2 depletion by microbial respiration at mid-water depths below the euphotic zone [25–27]. Here, shallow (< 300 m depth) near-shore waters above the continental shelf may be highly O_2-depleted ($O_2 < 5$ μM), while offshore waters above the continental slope experience milder subsurface hypoxia ($O_2 < 60$ μM) [7,12,28,30].

Such variation in O_2 levels may influence the coupling of NO_2^- production and consumption. In an analysis of offshore, deeper Benguela sites (seabed depth $> 1{,}000$ m at most sites), Mashifane et al. (2016) detected a primary NO_2^- maximum only in the oxic euphotic zone (30–50 m), which was attributed to a decoupling of nitrification steps and/or microbial assimilatory NO_3^- reduction to NO_2^-, but did not detect a secondary NO_2^- maximum at deeper depths. In contrast, near-shore sites (seabed depth ~100 m to ~300 m) on the Namibia shelf exhibit NO_2^- maxima at hypoxic (generally defined as $\leq$ ~60–120 μM [31]) or anoxic depths (where O_2 is near or below detection limits, ~10 nM to 1–2 μM depending on sensor technology), typically below ~50–80 m depth [7,12,23,29], a feature common in O_2-deficient waters where high rates of NO_3^- reduction drive NO_2^- accumulation [18,26,32]. At these near-shore sites, NO_2^- oxidation rates have been shown to exceed those of NH_3 oxidation, and NOB, roughly evenly represented by the genera *Nitrospina* and *Nitrococcus*, may constitute up to 10% of the total community [7]. These results, alongside those of others [29], suggest active nitrification in near-shore waters above the Namibian shelf, with the balance of NO_2^- also strongly influenced by anaerobic metabolisms, including NO_2^--consuming anammox.

It remains less clear how nitrifier community composition and coupling of NO_2^- consumption and production by nitrifiers change upon the transition to the O_2-enriched (but still hypoxic) waters further offshore in the Benguela system. Studies in other systems indicate that AOA distributions and NH_3 oxidation rates are influenced by nutrient and O_2 concentrations [33–35], and that AOA communities in the Arabian Sea OMZ are distinct from those of OMZs of the Eastern Pacific [36]. A study of relatively O_2-rich waters in Monterey Bay and the North Pacific Subtropical Gyre showed that the ratio of AOA to NOB ranged from 5:1 to 1:1 [37], suggesting a coupling of ammonia oxidizers and NOB. Similarly, a study in oxic waters of the Gulf of Mexico found that AOA outnumbered NOB by 20 to 1 [38]. The relative abundances of these groups were correlated and secondary NO_2^- maxima were not observed, which together was interpreted as a coupling between nitrifiers [38]. In contrast, Bristow et al. (2015) reported NO_2^- accumulation in hypoxic waters (~16–60 μM), while recording a similarly disproportionate relationship between AOA and NOB abundance, and a decoupling of NH_3 and NO_2^- oxidation rates at sites spanning hypoxic to oxic conditions on the Louisiana Shelf. Such studies indicate that nitrifier community structuring is dynamic based on environment and geography, and our current limited understanding of whether the relative abundances of ammonia and nitrite oxidizers are predictive of nitrifier coupling.

To explore variation in nitrifier community structuring and coupling, we assessed the relative abundances, phylogenetic diversity, and co-occurrence of nitrifying taxa offshore of Namibia. Using 16S rRNA amplicon gene sequencing, we analyzed the nitrifier community at five depths spanning oxic to hypoxic conditions, while measuring temperature and O_2, NO_2^-, and N_2O concentrations. We hypothesized that ammonia and nitrite oxidizer diversity changes with depth and decreasing O_2 concentrations, NOB community composition differs from that previously described at more O_2-depleted sites close to shore, and ammonia oxidizer to NOB ratios help predict NO_2^- accumulation. Testing these hypotheses sheds light on the environmental drivers of nitrifier community structure and how these communities may influence N availability.

Materials and methods

Site description, geochemical profiles, seawater sample collection

Seawater samples from the Northern Benguela Upwelling system off the Namibian coast were collected during cruise M-103 (“NAMUFil”; Dec. 27, 2013 –Feb. 11, 2014) of the R/V *Meteor*. All cruise operations were conducted in accordance with the Namibian Ministry of Foreign Affairs and Ministry of Mines and Energy. No additional permissions were required for seawater sampling. Samples for microbial analysis were collected on January 31, 2014 at station 116 (20.172˚S, 11.540˚E) over the continental slope (water depth ~865 m) approximately 150 km from the coast. Seawater was obtained from depths of 10, 25, 100, 130, and 250 m using a rosette equipped with a conductivity, temperature, and depth sensor (CTD), fluorometer (Wet Labs ECO-AFL/FL), and SBE 9 dissolved oxygen sensor (Sea-Bird Scientific). Four liters of water per depth (station 116) were filtered through a 0.22 μm-pore size 47 mm polycarbonate Nuclepore filter (Whatman). Filters were frozen immediately and stored at −80˚C. Using water from a separate hydrocast on January 31, 2014, samples for measuring N_2O were collected from 15 depths (17 to 250 m; Fig 1B). For each, water was twice overfilled into 160 ml glass bottles and preserved by adding 5 ml of 10 M sodium hydroxide [39], followed by vigorous shaking. Within 3 months of collection, total N_2O in each bottle (one per depth) was purged with carrier helium into a purge- and-trap system [40] and analyzed by continuous-flow gas chromatography-isotope ratio mass spectrometry (GC-IRMS) was previously described [41], with atmospheric equilibrium N_2O concentrations calculated using the

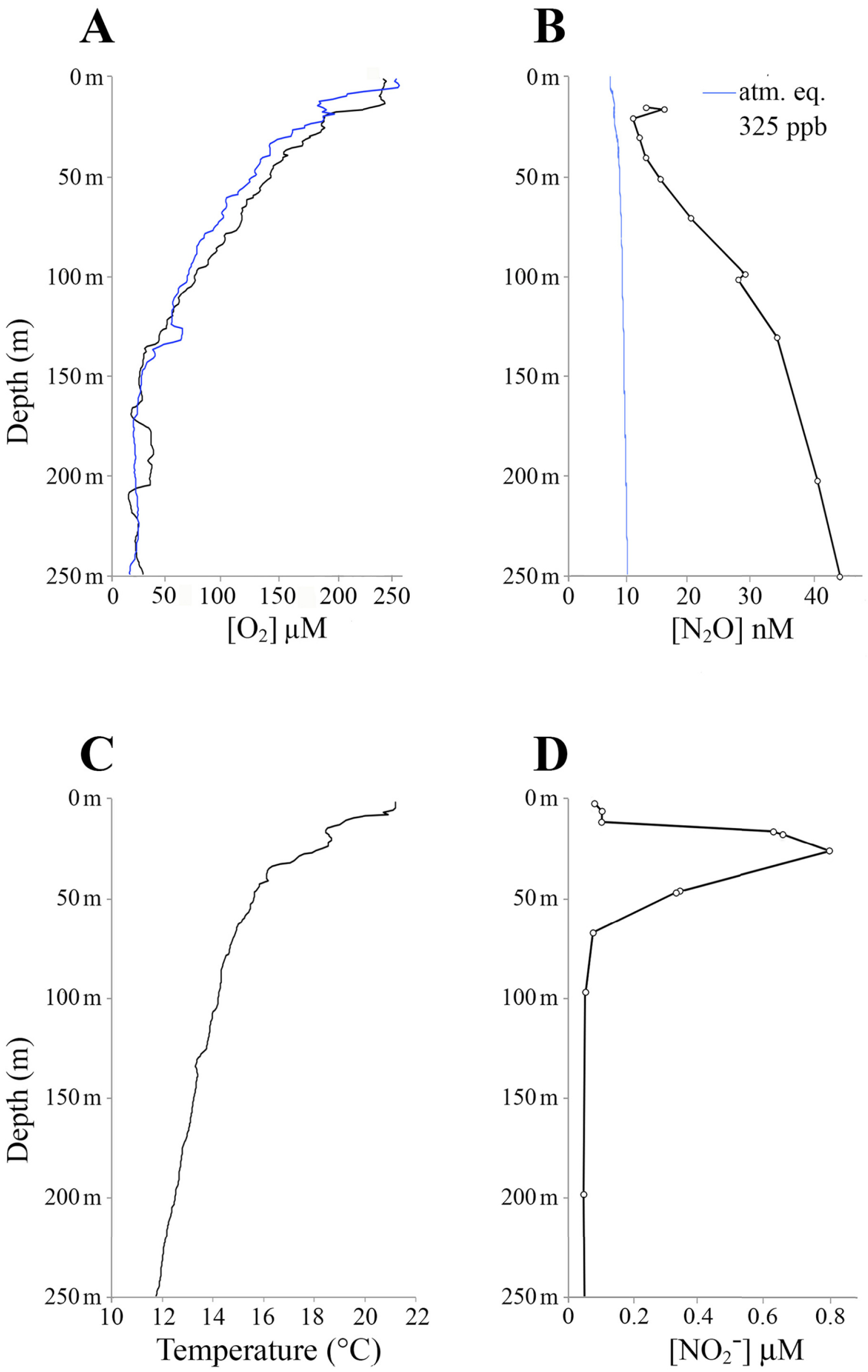
A
0 m
50 m
100 m
150 m
200 m
250 m
Depth (m)
0 50 100 150 200 250
$[O_2]$ µM
B
atm. eq. 325 ppb
0 10 20 30 40
$[N_2O]$ nM
C
10 12 14 16 18 20 22
Temperature (°C)
D
0 0.2 0.4 0.6 0.8
$[NO_2^-]$ µM

Fig 1. Environmental conditions at the study sites in January 2014. (A) O_2 concentration at stations 116 (blue line) and 117 (black line), (B) N_2O concentration at station 116 (black line), with concentration of dissolved N_2O at equilibrium (blue line), (C) temperature at station 116, and (D) NO_2^- concentration at station 117. Microbial samples were collected at station 116. Stations 116 and 117 are separated by ~10 km.

https://doi.org/10.1371/journal.pone.0217136.g001

solubility coefficients of Weiss and Price (1980), assuming a 325 ppb atmospheric mole fraction [42]. NO_2^- concentrations were not measured at station 116. However, NO_2^- was measured in samples (12 depths; 0 to 300 m; Fig 1D) collected on February 1, 2014 from station 117 (20.204˚S, 11.444˚E), approximately 10 km west-southwest of station 116. NO_2^- in 10 ml of sample was measured by converting NO_2^- to N_2O by azide reduction [43], followed by N_2O measurement via GC-IRMS as above. Calculations of N_2O and NO_2^- concentrations were previously described [41].

16S rRNA gene amplicon sequencing

The composition of the prokaryotic microbial community was assessed via 16S rRNA gene amplicon sequencing. Briefly, DNA was extracted using the FastDNA spin kit for soil (MP Biomedicals) following the manufacturer's protocol. The polymerase chain reaction was used to amplify the V4 region of the 16S rRNA gene using barcoded universal primers F515 (`5′- GTG CCAGCMGCCGCGGTAA-3′`) and R806 (`5′-GGACTACHVGGGTWTCTAAT-3′`) [44] appended with Illumina-specific adapters [45], with PCR run for 30 cycles using previously described thermal cycler protocol [46]. Three replicate PCR amplifications (different barcodes) were conducted for each of the five depths (15 total reactions). Gel electrophoresis was used to separate PCR products, which were then excised and recovered using a QIAquick gel extraction kit (Qiagen). The amplicon pool was then sequenced on an Illumina MiSeq at the West Virginia University Genomics Core Facility using V2 sequencing reagents, generating paired reads of ∼250 bp, with ∼150 bp overlap between forward and reverse reads.

Bioinformatic analyses

Paired read merging, quality filtering and denoising, and assignment and analysis of operational taxonomic units (OTUs) were carried out using PANDAseq in Axiome [47,48] and the Quantitative Insights Into Microbial Ecology (QIIME v.1.8.0) pipeline (Caporaso et al., 2010). In PANDAseq, the minimum overlap length was set at 0.9 and the read length maximum was set at 253 bp. Reads were removed from analysis if at least one of the following criteria was met: reads were $>$ 4 bp shorter than the maximum (253 bp), the number of ambiguous bases was $>$ 1, homopolymers with $>$ 4 bp were present, or sequences did not match any sequences in the database at $>$ 97% coverage via BLAST [49]. In QIIME, sequences were clustered into OTUs at 97% sequence identity using UCLUST [50,51], with OTU taxonomic classification done using the RDP classifier [52] at a confidence threshold of 70% and Greengenes datafiles gg_13_8 compiled in May 2013 (http://greengenes.lbl.gov). This step included chimera screening based on 16S rRNA genes in GenBank [53]. All OTUs matching known AOA, AOB, NOB, and MOB (methane oxidizing bacteria) were retrieved and their taxonomic assignments further verified via BLASTN against the NCBI 16S rRNA sequence database (for Bacteria + Archaea).

Phylogenetic analysis of 16S rRNA sequences

Phylogenetic trees were constructed using MEGA 7 [54]. The 16S rRNA gene sequences of representative AOA, AOB, NOB, and MOB were downloaded from GenBank [55]. To verify that 16S rRNA gene sequences were indeed nitrifiers or MOB, sequences were removed if they shared $\leq$ 80% identity with known AOA, AOB, NOB, and MOB based on BLAST search. Gene sequences were aligned using MUSCLE in MEGA 7 and manually inspected. The final alignments for AOA, AOB, NOB, and MOB comprised 794, 36, 338, and 27 taxa, respectively. Phylogenetic reconstruction was implemented using Maximum Likelihood (ML), employing the Tamura-Nei model of nucleotide substitution rate, with tree inference based on Nearest-Neighbor-Interchange. Statistical support for ML trees was obtained from 1,000 bootstrap replicates under the initial settings (only bootstrap values $>$ 50% are reported). Rarefaction curves using only ammonia oxidizer (AOA+AOB) OTUs and NOB OTUs were generated using the vegan package in R [56] to estimate nitrifier species richness.

Statistical and ecological analyses, diversity indices

Nitrifier and MOB OTU frequencies (proportional abundances) were determined using a Python (v.2.7) script to count all OTUs verified by the above phylogenetic analyses, as previously described [41,57]. The Shannon-Weiner diversity and Pielou (J) evenness indices were calculated using the BiodiversityR package [58] in R version 3.4.1 (http://www.R-project.org/). Correlation between nitrifier (AOA+AOB and NOB) diversity indices or OTU abundances and geochemical measurements (O_2, NO_2^-, N_2O concentrations, and temperature) at all 5 depths were calculated in R using the adjusted R-squared coefficient of determination.

To identify nitrifier OTUs that co-occurred at the same depth, hierarchical cluster analysis was performed using a Euclidean distance matrix based on ammonia oxidizer and NOB frequencies at each depth (after omitting depths where any given OTU occurred only once), generated in R version 3.5.0 (https://CRAN.R-project.org/package=ggdendro). Using this distance matrix and the "agnes" function in the "cluster" package (https://cran.r-project.org/web/packages/cluster/index.html), agglomerative clustering was performed using Ward's minimum variance method, chosen to minimize overall within-cluster variance. The results were visualized using the packages "ggplot2" [59] and "ggdendro" [60].

Project and sequence accession numbers

All sequence data are available through the European Bioinformatics Institute (EBI) under project accession number PRJEB21239 and individual accession numbers LT896734–LT897482 for ammonia-oxidizing microbes, LT897483–897776 and LT900516 for NOB, and LT900504–900514 for MOB (S1–S4 Tables).

Results

Geochemical profiles

Dissolved O_2 concentration at station 116 declined from 252 μM at the surface to 64 μM (or ~2 mg L^{-1}, the beginning of hypoxia) at 105 m depth, declining to a minimum of ~20–25 μM from ~170 m to 370 m (Fig 1A, S1 Fig). Below 370 m, O_2 concentration increased gradually to ~120 μM just above the sediment-water interface (S1 Fig). N_2O concentration increased steadily from ~10–20 nM in the oxic zone to $>$ 30 nM at hypoxic depths below 80 m, peaking at ~40 nM at 250 m (Fig 1B). Seawater temperature declined from 21°C at the surface to 12°C at 250 m (Fig 1C). Fluorescence peaked at ~3.9 mg m^{-3} at 10 m and declined to near zero by 80 m (S2 Fig). NO_2^- was not measured at station 116. At station 117, ~10 km from station 116 and with similar O_2 concentration profile as station 116 (Fig 1A), NO_2^- concentration exhibited a primary maximum (up to 0.8 μM) between 20 m and 50 m, and was consistently low ($<$ 0.1 μM) in the hypoxic zone (Fig 1D), which occurred at roughly the same depths as at station 116; a secondary NO_2^- maximum was not observed.

Counts of 16S rRNA gene amplicons (after quality filtering) ranged from 9,681 to 945,184 across the 15 datasets (5 depths X 3 triplicate PCR reactions per depth). Average OTU counts per dataset ranged from 4,912 to 8,312. At this sequence depth, the observed OTU counts represented 20.0%–60.7% (mean = 47.8%) of the OTU counts estimated via Chao1 (see rarefaction curves in S3 Fig).

Of the total OTUs classified across all samples using the RDP classifier in QIIME, 747 were affiliated with AOA, 2 were affiliated with AOB, 295 were affiliated with NOB, and 11 were affiliated with MOB. The taxonomic assignment of these OTUs was further verified via BLASTN (against NCBI) and phylogenetic analysis. All 747 AOA OTUs had top BLASTN matches (88%–100% identity) to AOA of the Thaumarchaeota (S1 Table), with 745 of these having top matches to strains of the open ocean archaeon *Candidatus* Nitrosopelagicus brevis or to *Nitrosopumilus* spp. of the family Nitrosopumilaceae. The majority (57.8%) clustered into OTUs most similar (94%–100%) to *Ca*. N. brevis CN25 (S1 Table), a pelagic AOA member adapted to the oligotrophic surface ocean [61]. The remaining 2 AOA OTUs matched *Nitrososphaera* sp. of the family Nitrososphaeraceae, which thus far primarily includes representatives from soils (S1 Table) [62]. Phylogenetic analysis supported the AOA classification; all AOA OTUs clustered in a broad clade with diverse Thaumarchaeota (71% bootstrap support). Within this clade, however, OTU placement was not well resolved, likely due to the low information content of the short 16S rRNA gene sequences (Fig 2).

Consistent with RDP classification, the 2 AOB OTUs matched AOB of the Nitrosomodaceae, sharing 89%–94% identity to *Nitrosospira briensis* C-128 from soil (S2 Table) [63]. These 2 OTUs grouped within a diverse but not well-supported (60% bootstrap support) clade of betaproteobacterial AOB, but represented two distinct lineages within this clade (Fig 3).

Of the 295 NOB OTUs, 291 had top BLASTN matches (87%–100% identity) to *Nitrospina* spp. of the phylum Nitrospinae, with over 80% of these being most similar to *Nitrospina gracilis* strain 3/211 (NR_104821.1) or *Nitrospina gracilis* (Atlantic Ocean isolate) (L35504.1) (S3 Table). These OTUs clustered unambiguously (99% bootstrap support) within the Nitrospinaceae but could not be resolved further within this clade (Fig 4). The remaining 4 NOB OTUs matched the phylum Nitrospirae, sharing 94%–98% identity with *Nitrospira* sp. enrichment culture clone LD3 from forest soil and *Nitrospira* sp. enrichment culture clone LPTV-S11 from a marine sponge (S3 Table) [64], and represented multiple lineages within the Nitrospirae clade (Fig 4).

Analysis of the 11 MOB OTUs identified 6 OTUs with top BLASTN matches (90%–97% identity) to the gammaproteobacterial family Methylococcaceae and 5 with matches (83%–84% identity) to the Verrucomicrobia family Methylacidiphilaceae (S4 Table). Phylogenetic analysis confirmed the family-level MOB classifications and also showed that these OTUs represent multiple lineages within each family (S5 Fig).

Nitrifier abundance and distribution

Nitrifier relative abundances varied substantially with depth (S4 Fig). Notably, AOA sequences affiliated with Thaumarchaeota sequences increased from ~1% of total sequences at 10 m to 33% at 130 m, before declining slightly to 25% at 250 m (S4 Fig). In contrast, AOB were largely absent; the ratio of AOA to AOB sequences exceeded 90,000:1 at all depths where AOB were detected (only at 25 m, 100 m, and 130 m; S2 Table). Similarly, AOA sequences substantially outnumbered nitrite oxidizer sequences at all depths. The ratio of ammonia (AOA+AOB) to nitrite oxidizer sequences was 41:1 at 10 m, but declined with depth to under 27:1 at 250 m (Table 1). Along this depth gradient, sequences matching the NOB phylum Nitrospinae increased from 0% at 10 m to 0.9% at 250 m, representing $>$ 99.9% of all NOB counts at all

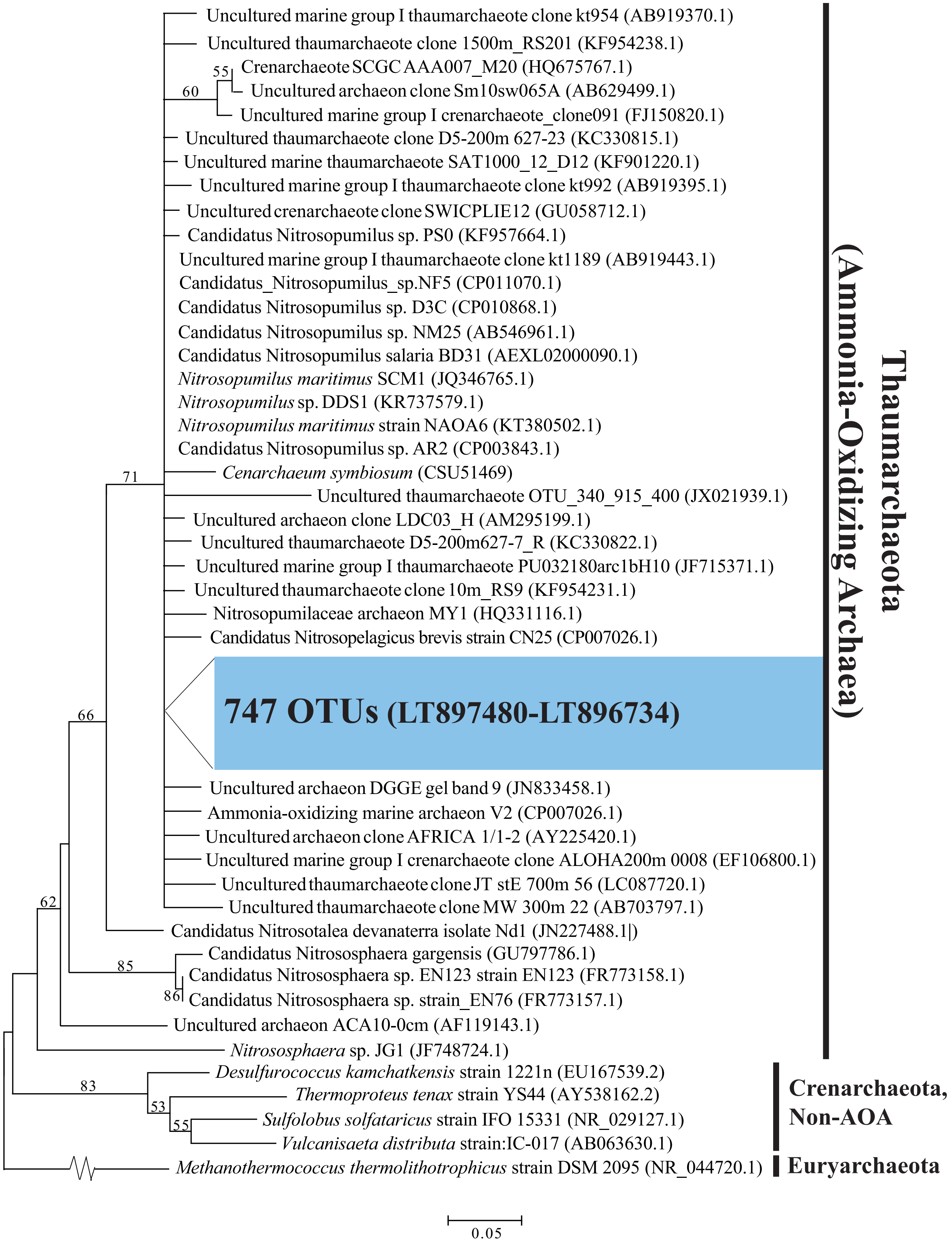
Uncultured marine group I thaumarchaeote clone kt954 (AB919370.1)
Uncultured thaumarchaeote clone 1500m_RS201 (KF954238.1)
55
Crenarchaeote SCGC AAA007_M20 (HQ675767.1)
60
Uncultured archaeon clone Sm10sw065A (AB629499.1)
Uncultured marine group I crenarchaeote_clone091 (FJ150820.1)
Uncultured thaumarchaeote clone D5-200m 627-23 (KC330815.1)
Uncultured marine thaumarchaeote SAT1000_12_D12 (KF901220.1)
Uncultured marine group I thaumarchaeote clone kt992 (AB919395.1)
Uncultured crenarchaeote clone SWICPLIE12 (GU058712.1)
Candidatus Nitrosopumilus sp. PS0 (KF957664.1)
Uncultured marine group I thaumarchaeote clone kt1189 (AB919443.1)
Candidatus_Nitrosopumilus_sp.NF5 (CP011070.1)
Candidatus Nitrosopumilus sp. D3C (CP010868.1)
Candidatus Nitrosopumilus sp. NM25 (AB546961.1)
Candidatus Nitrosopumilus salaria BD31 (AEXL02000090.1)
Nitrosopumilus maritimus SCM1 (JQ346765.1)
Nitrosopumilus sp. DDS1 (KR737579.1)
Nitrosopumilus maritimus strain NAOA6 (KT380502.1)
Candidatus Nitrosopumilus sp. AR2 (CP003843.1)
71
Cenarchaeum symbiosum (CSU51469)
Uncultured thaumarchaeote OTU_340_915_400 (JX021939.1)
Uncultured archaeon clone LDC03_H (AM295199.1)
Uncultured thaumarchaeote D5-200m627-7_R (KC330822.1)
Uncultured marine group I thaumarchaeote PU032180arc1bH10 (JF715371.1)
Uncultured thaumarchaeote clone 10m_RS9 (KF954231.1)
Nitrosopumilaceae archaeon MY1 (HQ331116.1)
Candidatus Nitrosopelagicus brevis strain CN25 (CP007026.1)
66
747 OTUs (LT897480-LT896734)
Uncultured archaeon DGGE gel band 9 (JN833458.1)
Ammonia-oxidizing marine archaeon V2 (CP007026.1)
Uncultured archaeon clone AFRICA 1/1-2 (AY225420.1)
Uncultured marine group I crenarchaeote clone ALOHA200m 0008 (EF106800.1)
Uncultured thaumarchaeote clone JT stE 700m 56 (LC087720.1)
Uncultured thaumarchaeote clone MW 300m 22 (AB703797.1)
62
Candidatus Nitrosotalea devanaterra isolate Nd1 (JN227488.1|)
Candidatus Nitrososphaera gargensis (GU797786.1)
85
Candidatus Nitrososphaera sp. EN123 strain EN123 (FR773158.1)
86
Candidatus Nitrososphaera sp. strain_EN76 (FR773157.1)
Uncultured archaeon ACA10-0cm (AF119143.1)
Nitrososphaera sp. JG1 (JF748724.1)
Desulfurococcus kamchatkensis strain 1221n (EU167539.2)
83
Thermoproteus tenax strain YS44 (AY538162.2)
53
55
Sulfolobus solfataricus strain IFO 15331 (NR_029127.1)
Vulcanisaeta distributa strain:IC-017 (AB063630.1)
Methanothermococcus thermolithotrophicus strain DSM 2095 (NR_044720.1)
Thaumarchaeota (Ammonia-Oxidizing Archaea)
Crenarchaeota, Non-AOA
Euryarchaeota
0.05

Fig 2. Phylogenetic relationships among ammonia-oxidizing archaea (AOA) of the Thaumarchaeota. The tree is based on maximum likelihood (ML) analysis of 747 OTUs ($\sim$253 bp) detected in this study (in blue), compared to close relatives. Accession numbers are indicated in parentheses. Bootstrap values from 1000 replicates are indicated at the nodes of branches (if > 50). The scale bar represents the number of substitutions per site.

https://doi.org/10.1371/journal.pone.0217136.g002

depths sampled, whereas those of the phylum Nitrospirae comprised $< 0.1\%$ (S4 Fig; S3 Table). NOB sequences matching *Nitrococcus*, *Nitrobacter*, or *Nitrotoga* were not detected. The percentage abundance of both the ammonia oxidizer community was weakly correlated with dissolved O_2 concentration and temperature with the relationship being strongest for the NOB community ($r = -0.81$ for correlations with O_2 and temperature, respectively; $p < 0.1$; S5 Table). MOB sequences were rare, constituting less than 0.0005% of all sequences at all depths (S4 Table).

Nitrifier community structure varied with sample depth in our analyses of sequence reads from 5 depths at one site. The OTU richness (observed), diversity (*H*; Shannon-Weiner index), and evenness (*J*; Pielou's index) of both the ammonia oxidizer (AOA+AOB) and NOB communities increased consistently with depth from the surface to the hypoxic zone (Fig 1, Fig 5, S4 Fig) and regression analysis indicated strong positive linear correlation between the *H* indices of AOA+AOB and NOB ($r = 0.99$) (S7 Fig). These trends differ from that of the total microbial community (all OTUs considered), in which richness was highest at the shallowest depths (10 m and 25 m; S4 Fig), and were most dramatic in the ammonia oxidizer community. Notably, the observed number of ammonia oxidizer OTUs (the overwhelming majority of which were AOA; see above) more than doubled from 25 m to 250 m (S6A Fig; evaluated at a common sequence depth of 150,000) and evenness increased by roughly 50% with depth (Fig 5), indicating a shift to a more equal representation of community members (fewer dominant taxa) from the surface to the hypoxic zone.

Most nitrifier OTUs were not detected broadly across all depths. Whereas 65% of ammonia oxidizer OTUs and 55% of NOB OTUs were detected at more than one depth, only 5% of ammonia oxidizer OTUs and 4% of NOB OTUs were detected at all 5 depths (S1 and S3 Tables). A subset of AOA OTUs {n = 22; marked with an asterisk (*) in S1 Table} was detected in at least 4 depths but was substantially enriched at the shallowest depths, collectively representing 84% and 94% of ammonia oxidizer reads at 10 m and 25 m, respectively, but only 21%, 2% and $< 1\%$ at 100 m, 130 m, and 250 m, respectively. Furthermore, hierarchical cluster analysis identified 55 AOA and 52 NOB (all placed within the genus *Nitrospina*) OTUs that were placed in 12 groups based on co-occurrence patterns (S6 Table).

Discussion

Our data from an offshore site in the Benguela Upwelling system identified a prominent nitrifier community whose taxonomic composition varied substantially with depth, and in comparison to prior results from closer to the coast [7]. Consistent with studies showing AOA dominance over AOB in marine systems [1,18,38,65–70], the ammonia oxidizer community at station 116 was composed almost exclusively of Thaumarchaeota (AOA). AOA abundance increased from ~1% at oxic depths to up to 33% in the hypoxic zone, suggesting ammonia as a substantial energy source. In contrast, the NOB community, composed primarily of *Nitrospina*, never accounted for more than 1% of sequences. However, like the AOA, NOB abundance increased with depth. At depths of peak AOA and NOB abundance, O_2 concentrations were low (~20–70 μM) compared to the surface but still considerably higher than levels known to inhibit anaerobic metabolisms such as denitrification and anammox (hundreds of nM to low μM) [e.g., 12,17,79]. Rather, minimum O_2 levels at stations 116 and 117 were within the

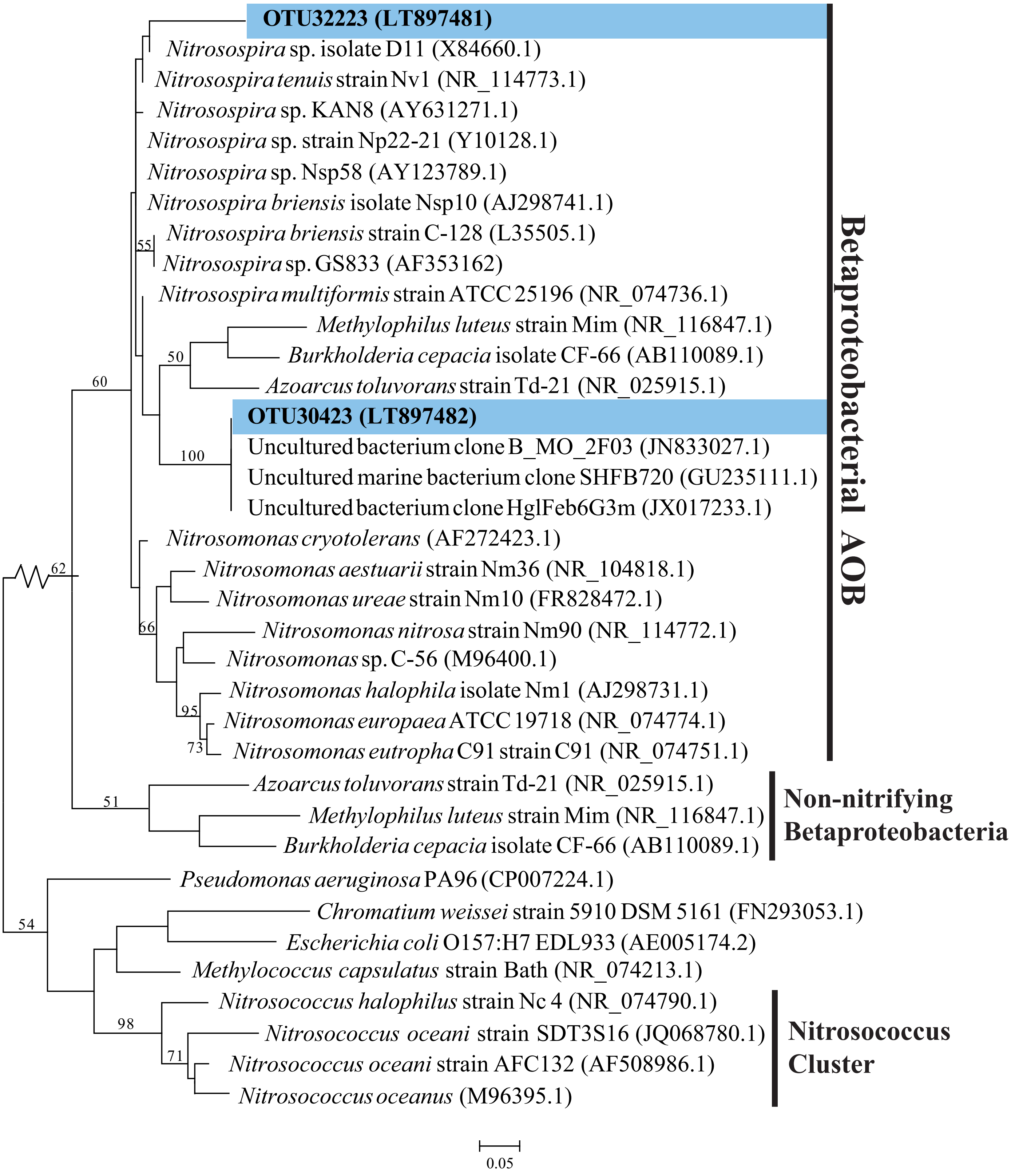
OTU32223 (LT897481)
Nitrosospira sp. isolate D11 (X84660.1)
Nitrosospira tenuis strain Nv1 (NR_114773.1)
Nitrosospira sp. KAN8 (AY631271.1)
Nitrosospira sp. strain Np22-21 (Y10128.1)
Nitrosospira sp. Nsp58 (AY123789.1)
Nitrosospira briensis isolate Nsp10 (AJ298741.1)
55
Nitrosospira briensis strain C-128 (L35505.1)
Nitrosospira sp. GS833 (AF353162)
Nitrosospira multiformis strain ATCC 25196 (NR_074736.1)
Methylophilus luteus strain Mim (NR_116847.1)
50
Burkholderia cepacia isolate CF-66 (AB110089.1)
60
Azoarcus toluvorans strain Td-21 (NR_025915.1)
OTU30423 (LT897482)
100
Uncultured bacterium clone B_MO_2F03 (JN833027.1)
Uncultured marine bacterium clone SHFB720 (GU235111.1)
Uncultured bacterium clone HglFeb6G3m (JX017233.1)
Nitrosomonas cryotolerans (AF272423.1)
62
Nitrosomonas aestuarii strain Nm36 (NR_104818.1)
Nitrosomonas ureae strain Nm10 (FR828472.1)
66
Nitrosomonas nitrosa strain Nm90 (NR_114772.1)
Nitrosomonas sp. C-56 (M96400.1)
Nitrosomonas halophila isolate Nm1 (AJ298731.1)
95
Nitrosomonas europaea ATCC 19718 (NR_074774.1)
73
Nitrosomonas eutropha C91 strain C91 (NR_074751.1)
Betaproteobacterial AOB
Azoarcus toluvorans strain Td-21 (NR_025915.1)
51
Methylophilus luteus strain Mim (NR_116847.1)
Burkholderia cepacia isolate CF-66 (AB110089.1)
Non-nitrifying Betaproteobacteria
Pseudomonas aeruginosa PA96 (CP007224.1)
Chromatium weissei strain 5910 DSM 5161 (FN293053.1)
54
Escherichia coli O157:H7 EDL933 (AE005174.2)
Methylococcus capsulatus strain Bath (NR_074213.1)
Nitrosococcus halophilus strain Nc 4 (NR_074790.1)
98
Nitrosococcus oceani strain SDT3S16 (JQ068780.1)
71
Nitrosococcus oceani strain AFC132 (AF508986.1)
Nitrosococcus oceanus (M96395.1)
Nitrosococcus Cluster
0.05

Fig 3. Phylogenetic relationships among ammonia-oxidizing bacteria (AOB). The tree is based on maximum likelihood (ML) analysis of 2 OTUs (~253 bp) detected in this study (in blue), compared to relatives from the Nitrosomonadaceae (Betaproteobacteria). Accession numbers are indicated in parentheses. Bootstrap values from 1000 replicates are indicated at the nodes of branches (if > 50). The scale bar represents the number of substitutions per site.

https://doi.org/10.1371/journal.pone.0217136.g003

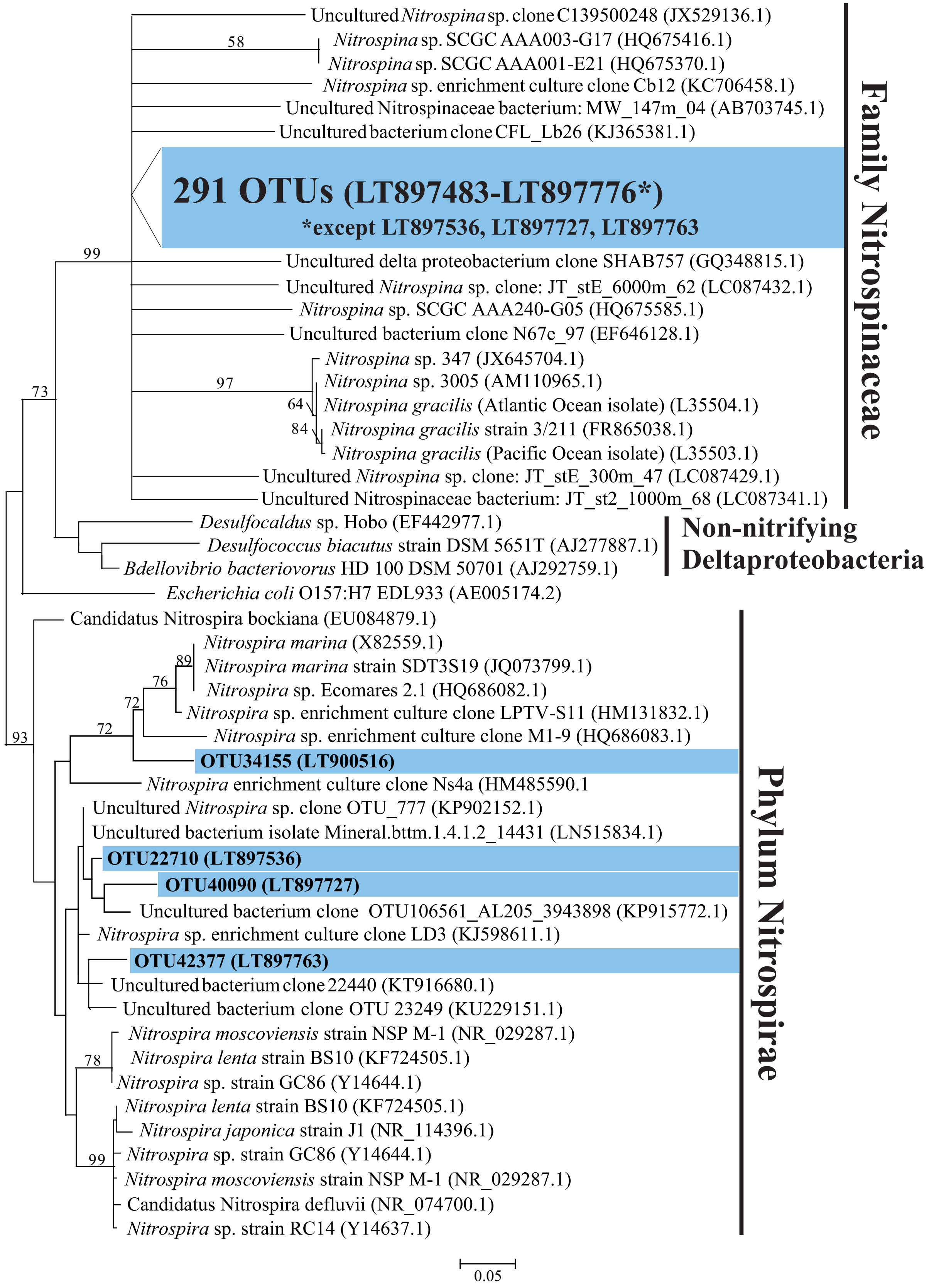
Uncultured *Nitrospina* sp. clone C139500248 (JX529136.1)
58
Nitrospina sp. SCGC AAA003-G17 (HQ675416.1)
Nitrospina sp. SCGC AAA001-E21 (HQ675370.1)
Nitrospina sp. enrichment culture clone Cb12 (KC706458.1)
Uncultured Nitrospinaceae bacterium: MW_147m_04 (AB703745.1)
Uncultured bacterium clone CFL_Lb26 (KJ365381.1)
291 OTUs (LT897483-LT897776*)
***except LT897536, LT897727, LT897763**
99
Uncultured delta proteobacterium clone SHAB757 (GQ348815.1)
Uncultured *Nitrospina* sp. clone: JT_stE_6000m_62 (LC087432.1)
Nitrospina sp. SCGC AAA240-G05 (HQ675585.1)
Uncultured bacterium clone N67e_97 (EF646128.1)
Nitrospina sp. 347 (JX645704.1)
97
Nitrospina sp. 3005 (AM110965.1)
73
64
Nitrospina gracilis (Atlantic Ocean isolate) (L35504.1)
84
Nitrospina gracilis strain 3/211 (FR865038.1)
Nitrospina gracilis (Pacific Ocean isolate) (L35503.1)
Uncultured *Nitrospina* sp. clone: JT_stE_300m_47 (LC087429.1)
Uncultured Nitrospinaceae bacterium: JT_st2_1000m_68 (LC087341.1)
Family Nitrospinaceae
Desulfocaldus sp. Hobo (EF442977.1)
Desulfococcus biacutus strain DSM 5651T (AJ277887.1)
Bdellovibrio bacteriovorus HD 100 DSM 50701 (AJ292759.1)
Non-nitrifying Deltaproteobacteria
Escherichia coli O157:H7 EDL933 (AE005174.2)
Candidatus Nitrospira bockiana (EU084879.1)
Nitrospira marina (X82559.1)
89
Nitrospira marina strain SDT3S19 (JQ073799.1)
76
Nitrospira sp. Ecomares 2.1 (HQ686082.1)
72
Nitrospira sp. enrichment culture clone LPTV-S11 (HM131832.1)
93
72
Nitrospira sp. enrichment culture clone M1-9 (HQ686083.1)
OTU34155 (LT900516)
Nitrospira enrichment culture clone Ns4a (HM485590.1
Uncultured *Nitrospira* sp. clone OTU_777 (KP902152.1)
Uncultured bacterium isolate Mineral.bttm.1.4.1.2_14431 (LN515834.1)
OTU22710 (LT897536)
OTU40090 (LT897727)
Uncultured bacterium clone OTU106561_AL205_3943898 (KP915772.1)
Nitrospira sp. enrichment culture clone LD3 (KJ598611.1)
OTU42377 (LT897763)
Uncultured bacterium clone 22440 (KT916680.1)
Uncultured bacterium clone OTU 23249 (KU229151.1)
Nitrospira moscoviensis strain NSP M-1 (NR_029287.1)
78
Nitrospira lenta strain BS10 (KF724505.1)
Nitrospira sp. strain GC86 (Y14644.1)
Nitrospira lenta strain BS10 (KF724505.1)
Nitrospira japonica strain J1 (NR_114396.1)
99
Nitrospira sp. strain GC86 (Y14644.1)
Nitrospira moscoviensis strain NSP M-1 (NR_029287.1)
Candidatus Nitrospira defluvii (NR_074700.1)
Nitrospira sp. strain RC14 (Y14637.1)
Phylum Nitrospirae
0.05

Fig 4. Phylogenetic relationship among nitrite-oxidizing bacteria (NOB). The tree is based on maximum likelihood (ML) analysis of 295 OTUs (~253 bp) detected in this study (in blue), compared to relatives from the phyla Nitrospirae and Nitrospinae. Accession numbers are indicated in parentheses. Bootstrap values from 1000 replicates are indicated at the nodes of branches (if > 50). The scale bar represents the number of substitutions per site.

https://doi.org/10.1371/journal.pone.0217136.g004

range (tens of μM) known to support high rates of both ammonia and nitrite oxidation within or at the periphery of low-oxygen zones where both AOA and NOB have been found at high abundance [e.g., 7,12–14,36,71,72].

Given these conditions, we hypothesize that AOA activity was the main local biological source of both N_2O and NO_2^- in the hypoxic layer, and that NOB of the *Nitrospina* were the main biological NO_2^- sink. Indeed, the proportional increase in AOA with depth coincided with an increase in N_2O concentration to > 40 nM (Fig 1B), a level consistent with that reported previously for the area [30,73]. In contrast, NO_2^-, as measured at a nearby station 117 (~10 km away) with O_2 conditions similar to those at station 116 (Fig 1), reached a maximum only in the oxic photic zone (~25 m– 30 m) and a deeper secondary NO_2^- maximum was not observed. At station 116, AOA abundances were low in the photic depths, potentially due to competition with phytoplankton [74]. Assuming similar NO_2^- conditions existed at stations 116 and 117, then NO_2^- accumulation at upper depths was likely driven by processes other than AOA activity, potentially incomplete assimilatory NO_3^- reduction by phytoplankton [75]. Indeed, chloroplast genes represented 8–10% of 16S rRNA sequences at 10 and 25 m, coincident with high fluorescence values at these depths (S2 Fig). Given the concurrent increase in both AOA and NOB with depth, we propose that NO_2^- production by AOA became increasingly coupled to NO_2^- consumption by NOB beneath the primary NO_2^- maximum and into the hypoxic zone. Indeed, at station 116, the AOA:NOB ratio was highest in oxic depths (41:1) and lowest in the hypoxic zone (27:1). The lowest value was similar to that reported in a prior study (20:1) to suggest AOA:NOB coupling in the northern Gulf of Mexico [38]. Here, and in the prior study, an apparent coupling occurred even though NOB were rare compared to AOA. Indeed, the genomes of most *Nitrospina* sp. contain two rRNA operons [37]; thus, the true relative abundance of NOB may be lower than what we report. It is also likely that the bulk of ammonia oxidation proceeded through AOA and not through MOB, which can also oxidize NH_3 and thereby compete with ammonia oxidizers [76–78], but were barely detected in our data. A coupling between NO_2^- production (by AOA) and consumption would therefore suggest either disproportionately high oxidation rates by the minority NOB community, or alternative NO_2^- sinks.

These results provide a contrast to those of Füssel et al. (2012), which focused on sites closer to the coast on the Namibian Shelf (depths: 100 m– 130 m), where NO_2^- maxima (> 4 μM) coincided with O_2 levels (< 4 μM) considerably lower than those at our site. At such sites, NO_2^- accumulation is likely driven primarily by NO_3^- reduction, although low O_2-adapted AOA may also contribute to NO_2^- production [7,14,26]. Similarly, NO_2^- consumption by low

Table 1. Relative abundances of sequences matching ammonia-oxidizing microbes (AOA + AOB) and nitrite-oxidizing bacteria (NOB), expressed as a proportion of total sequences and as a ratio of (AOA+AOB) to NOB counts.

	AOA + AOB	NOB	C. (AOA+NOB):NOB
10 m	0.010	2.42×10^{-4}	41:1
25 m	0.251	0.006	40:1
100 m	0.245	0.006	39:1
130 m	0.309	0.009	34:1
250 m	0.249	0.009	27:1

https://doi.org/10.1371/journal.pone.0217136.t001

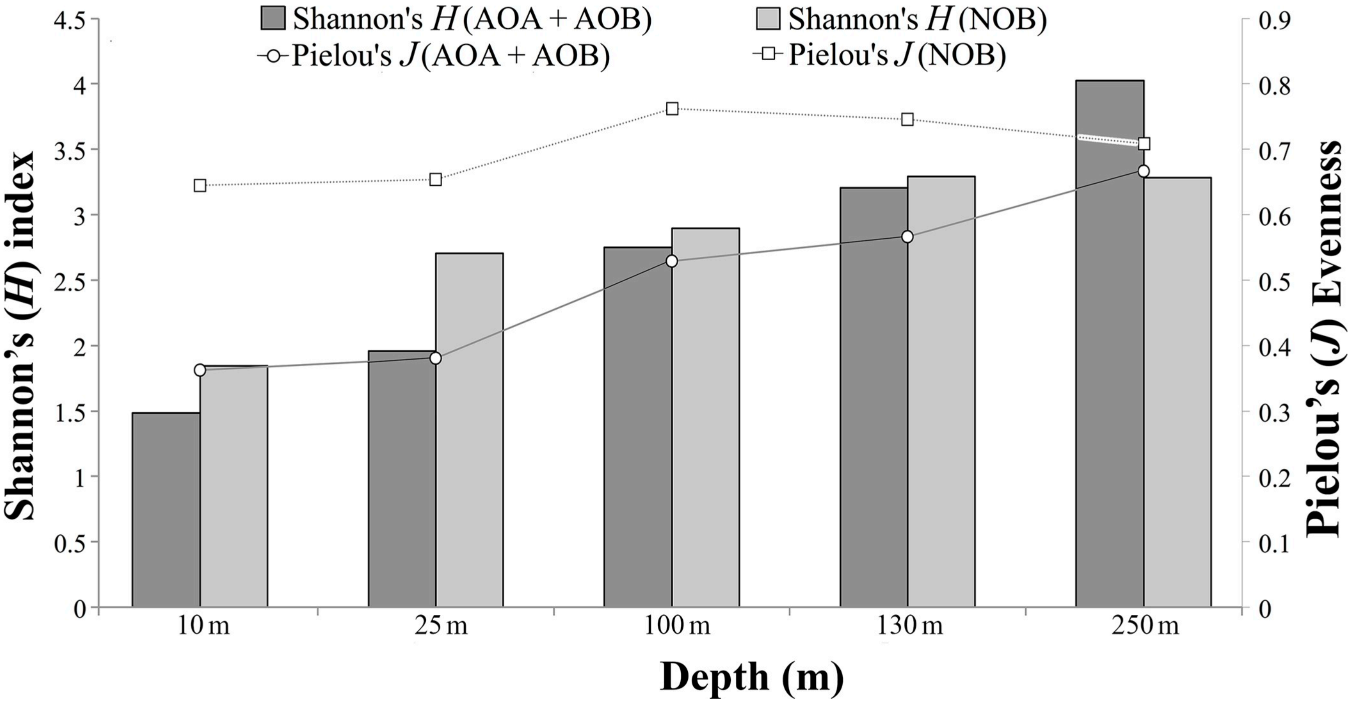

Fig 5. Diversity (*H*) and evenness (*J*) of ammonia-oxidizing (AOA + AOB) and nitrite-oxidizing (NOB) microbial communities. Depths of 10 and 25 m were in the oxic zone. Depths of 100, 130, and 250 m were in the hypoxic zone.

https://doi.org/10.1371/journal.pone.0217136.g005

O_2-adapted NOB may occur at such sites. Füssel et al. (2012) detected both *Nitrospina* and *Nitrococcus* NOB at up to ~5% (each) of the community at NO_2^--enriched depths and measured NO_2^- oxidation at rates exceeding those of NH_3 oxidation [7]. By comparison, *Nitrospina* and *Nitrospira* represented $> 99\%$ and $< 0.01\%$ of NOB counts at all depths, respectively, and we did not detect *Nitrococcus*. Rather, *Nitrospira* sequences, while present in our data (at low abundance) but not detected in Füssel et al. (2012), raising the hypothesis that *Nitrococcus* better tolerates low O_2 compared to *Nitrospira*. This is consistent with evidence suggesting diverse metabolic capabilities in *Nitrococcus*, including nitrate reduction and sulfide oxidation [8]. Füssel et al. (2012) also measured anammox rates comparable to, or exceeding those of NO_2^- oxidation at O_2-depleted depths [7], consistent with prior work indicating anammox as a major NO_2^- sink in O_2-deficient waters in this region [e.g., 29,80] and therefore as a potential competitor with NOB. In contrast, we did not detect anammox bacteria at station 116, where O_2 levels exceeded the upper limit for anammox [12,17,79]. Together, these results suggest that in the relatively O_2-enriched water over the continental slope, a proportionally less abundant (but potentially highly active) NOB community may balance NO_2^- production by AOA. In contrast, in more O_2-depleted waters closer to shore, the NOB community differs in composition and is at higher proportional abundance (versus overall microbial abundance) {~10% in Füssel et al. (2012) compared to 1% in our study}, but still insufficient to balance the combined NO_2^- production by AOA and nitrate reduction, even with concurrent NO_2^- consumption by anammox.

These results highlight variability in the nitrifier community with proximity to shore in the Benguela system. Variability is also evident over depth. Here, both the AOA and NOB communities exhibited lower evenness in oxic compared to hypoxic depths. This trend suggests that nitrification may proceed disproportionately through a minority of nitrifier taxa at oxic depths, but more uniformly through diverse nitrifier taxa at hypoxic depths. Notably, the subset of AOA OTUs (n = 22; S1 Table) that we identified as enriched (> 84% of sequences) in the upper depths may be the main contributors to ammonia oxidation in this zone. While our analysis suggests that many nitrifier OTUs occur across multiple depths, certain OTUs consistently co-occur with others (S6 Table), further suggesting non-random community structuring with depth. As O_2 levels fell, nitrifier richness and diversity (Shannon *H*), particularly in the AOA community, increased significantly (> 2-fold), to over 500 OTUs at hypoxic depths (S6A and S6B Fig); indeed, AOA diversity may be underestimated, as the PCR primers used in our study may exclude certain archaeal groups [81]. A similar inverse relationship between diversity and O_2 was observed at the periphery of Eastern Pacific OMZs, where total (nitrifier + non-nitrifier) microbial richness increased with depth and peaked at O_2 levels of ~10–15 μM [82]. However, the relationship between microbial diversity and O_2 is complex. At low to sub-μM O_2 levels, the relationship becomes positive, with diversity decreasing as O_2 decreases [82,83]. Further, the relationship differs among microbes; here, the negative relationship noted above for nitrifiers differs from the weak positive relationship observed for the entire community (S4 Fig). Together, these results suggest restructuring of nitrifier communities with depth, and potentially O_2 availability.

Despite their small volume in the oceans, oxygen deficient zones play a critical role in the oceanic N budget, with reductive microbial metabolisms at the core of these zones contributing 30%–50% of oceanic N loss [84,85]. These zones are expanding [31,86], making it critical to understand the microbial consequences of differing oxygen regimes. Oxygen conditions at our study site were intermediate between those of the oxic open ocean and the intensively O_2-depleted N loss zones closer to shore. Under these conditions, AOA appear to thrive and outnumber NOB by at least 25-fold. Yet NO_2^- does not accumulate, suggesting a tight coupling between the two nitrifying communities. It has been suggested that ammonia-oxidizing microbes and NOB may engage in physically close, syntrophic associations [87], with NOB presumably benefiting from NO_2^- supplied by AOA, and AOA (and/or AOB) benefiting from NOB activity, which prevents NO_2^- from accumulating to toxic concentrations [87–90]. Indeed, the co-occurrence between specific AOA and NOB OTUs (S6 Table) suggests potentially interacting taxa. Describing nitrifier diversity across geochemically variable sites remains a research priority [e.g., 7,9,10,11,14,34,36,67–69]. Alongside results from prior studies, our data inform a broad effort to predict how changing O_2 levels affect the structure and activity of the ocean N cycle.

Supporting information

S1 Fig. Complete dissolved O_2 profile for station 116, from surface to 860 m. Seabed depth: 862 m– 868 m.
(PDF)

S2 Fig. FIECO-AFL for station 116, from surface to 300 m.
(PDF)

S3 Fig. Microbial taxon richness at station 116, assessed by fifteen rarefaction curves (triplicate PCR amplifications for 5 different depths) for microbial OTUs in this study.
(PDF)

S4 Fig. Relative sequence abundances of archaeal and bacterial phyla or class based on the 833,468 unique OTU reads (out of 5,141,055 total reads) obtained from separate reactions in triplicate for each depth (10 m, 25 m, 100 m, 130 m, and 250 m) in the Namibian upwelling seawater at Station 116.
(PDF)

S5 Fig. Phylogenetic tree based on maximum likelihood (ML) analysis of 11 OTUs (~253 bp) of MOB and putative MOB detected in this study (in bold) in comparison with their close relatives and representatives from the families methyacidiphilaceae (phylum Verrucomicrobia) and Methylococcaceae (class gammaproteobacteria).
(PDF)

S6 Fig. Taxon richness from 10 m, 25 m, 100 m, 130 m, and 250 m depths, assessed by rarefaction curves for (A) ammonia oxidizer OTUs (AOA+AOB), and (B) nitrite oxidizer (NOB) OTUs in this study.
(PDF)

S7 Fig. Shannon diversity (*H*) of the AOA and AOB community compared to that of the NOB community.
(PDF)

S1 Table. Top named or cultured representative(s) based on BLASTN searches and read counts matching the 747 OTUs related to the ammonia-oxidizing archaea (AOA).
(PDF)

S2 Table. Top named or cultured representative(s) based on BLASTN searches and read counts matching the 2 OTUs related to the bacterial ammonia-oxidizing family Nitrosomodaceae.
(PDF)

S3 Table. Top named or cultured representative(s) based on BLASTN searches and read counts matching the 295 OTUs related to the bacterial nitrite-oxidizing family Nitrospinaceae and 4 OTUs related to the bacterial nitrite-oxidizing phylum Nitrospirae.
(PDF)

S4 Table. Top named or cultured representative(s) based on BLASTN searches and read counts matching the 6 OTUs related to MOB of the gammaproteobacterial family Methylococcaceae, and 5 OTUs related to MOB of the Verrucomicrobial family Methylacidiphilaceae.
(PDF)

S5 Table. Adjusted R (correlation coefficient) and *P* values in comparisons between nitrifier abundances (percentage of total sequences) versus temperature, dissolved O_2 concentration, and N_2O concentration.
(PDF)

S6 Table. Co-occurrence patterns of 55 AOA and 52 NOB OTUs.
(PDF)

Acknowledgments

We thank Ryan Percifeld and Neil Infante at West Virginia University for assistance with multiplex sequencing and Illumina® Basespace analyses, Michael Hall for assistance with debugging software and analyses, Sangita Ganesh, Neha Sarode and Fuhua Chen for assistance with protocol including barcoded 16S rRNA primers, QIIME and analyses, Thomas Auchtung and Anthony Bertagnolli for reading and commenting on the manuscript. Funding was provided by grants from the National Institutes of Health West Virginia IDeA Network of Biomedical Research Excellence (WV-INBRE, Award# 2P20GM103434-14), the West Liberty University

Faculty Development Fund, Swiss National Science Foundation Grant NUW1530, and the Freiwillige Akademische Gesellschaft of Basel, Switzerland.

Author Contributions

Conceptualization: Evan Lau, Caitlin H. Frame.

Data curation: Evan Lau, Caitlin H. Frame.

Formal analysis: Evan Lau, Caitlin H. Frame, E. Joseph Nolan IV, Daniel P. Lukich, Nicole E. Mihalik, Katelyn E. Yauch, Marcus A. Kinker.

Funding acquisition: Evan Lau, Caitlin H. Frame.

Investigation: Evan Lau, Caitlin H. Frame, E. Joseph Nolan IV, Zachary W. Dillard, Daniel P. Lukich, Nicole E. Mihalik, Katelyn E. Yauch, Marcus A. Kinker, Samantha L. Waychoff.

Methodology: Evan Lau, Caitlin H. Frame, E. Joseph Nolan IV, Frank J. Stewart.

Project administration: Evan Lau.

Resources: Evan Lau, Caitlin H. Frame, E. Joseph Nolan IV.

Software: Evan Lau, E. Joseph Nolan IV, Daniel P. Lukich.

Supervision: Evan Lau.

Validation: Evan Lau, Caitlin H. Frame, E. Joseph Nolan IV, Zachary W. Dillard, Daniel P. Lukich, Katelyn E. Yauch, Samantha L. Waychoff.

Visualization: Evan Lau, E. Joseph Nolan IV.

Writing – original draft: Evan Lau, Caitlin H. Frame, Frank J. Stewart.

Writing – review & editing: Evan Lau, Caitlin H. Frame, E. Joseph Nolan IV, Frank J. Stewart, Zachary W. Dillard, Daniel P. Lukich, Nicole E. Mihalik, Katelyn E. Yauch.

References

1. Wuchter C, Abbas B, Coolen MJ, Herfort L, van Bleijswijk J, Timmers P, et al. Archaeal nitrification in the ocean. Proc Nat Acad Sci. 2006; 103(33): 12317–12322. https://doi.org/10.1073/pnas.0600756103 PMID: 16894176
2. Brochier-Armanet C, Boussau B, Gribaldo S, Forterre P. Mesophilic Crenarchaeota: proposal for a third archaeal phylum, the Thaumarchaeota. Nat Rev Microbiol. 2008; 6(3):245–52. https://doi.org/10.1038/nrmicro1852 PMID: 18274537
3. Pester M, Schleper C, Wagner M. The Thaumarchaeota: an emerging view of their phylogeny and ecophysiology. Curr Opin Microbiol. 2011; 14(3): 300–306. https://doi.org/10.1016/j.mib.2011.04.007 PMID: 21546306
4. Watson SW, Bock E, Valois FW, Waterbury JB, Schlosser U. *Nitrospira marina* gen. Nov. sp. nov.: a chemolithotrophic nitrite-oxidizing bacterium. Arch Microbiol. 1986; 144(1):1–7. https://doi.org/10.1007/BF00454947
5. Spieck E, Bock E, The lithoautotrophic nitrite-oxidizing bacteria, in Bergey's Manual of Systematic Bacteriology, Garrity G., Brenner D. J., Krieg N. R., Staley J. R, Eds. (Springer-Verlag, ed. 2, 2005: 149–153.
6. Abeliovich A. The nitrite oxidizing bacteria. In: Dworkin M, Falkow S, Rosenberg E, Schleifer K-H, Stackebrandt E, editors. The Prokaryotes. New York: Springer; 2006; pp. 861–872.
7. Füssel J, Lam P, Lavik G, Jensen MM, Holtappels M, Günter M, et al. Nitrite oxidation in the Namibian oxygen minimum zone. ISME J. 2012; 6(6): 1200–1209. https://doi.org/10.1038/ismej.2011.178 PMID: 22170426
8. Füssel J, Lücker S, Yilmaz P, Nowka B, van Kessel MAHJ, Bourceau P, Hach PF, Littmann S, Berg J, Spieck E, Daims H, Kuypers MMM, Lam P. Adaptability as the key to success for the ubiquitous marine

nitrite oxidizer *Nitrococcus*. Sci Adv. 2017; 3(11): e1700807. https://doi.org/10.1126/sciadv.1700807 PMID: 29109973

9. Wankel SD, Mosier AC, Hansel CM, Paytan A, Francis CA. Spatial variability in nitrification rates and ammonia-oxidizing microbial communities in the agriculturally impacted Elkhorn Slough estuary, California. Appl Environ Microbiol. 2011; 77(1): 269–80. https://doi.org/10.1128/AEM.01318-10 PMID: 21057023

10. Biller SJ, Mosier AC, Wells GF and Francis CA. Global biodiversity of aquatic ammonia-oxidizing archaea is partitioned by habitat. Front Microbiol. 2012; 3: 252. https://doi.org/10.3389/fmicb.2012.00252 PMID: 22826704

11. Bristow LA, Sarode N, Cartee J, Caro-Quintero A, Thamdrup B. Stewart FJ. Biogeochemical and metagenomic analysis of nitrite accumulation in the Gulf of Mexico hypoxic zone. Limnol Oceanogr 2015; 60 (5): 1733–1750. https://doi.org/10.1002/lno.10130

12. Kalvelage T, Jensen MM, Contreras S, Revsbech NP, Lam P, Günter M, et al. Oxygen sensitivity of anammox and coupled N-cycle processes in oxygen minimum zones. PloS one. 2011; 6(12): e29299. https://doi.org/10.1371/journal.pone.0029299 PMID: 22216239

13. Beman JM, Shih JL, Popp BN. Nitrite oxidation in the upper water column and oxygen minimum zone of the eastern tropical North Pacific Ocean. ISME J, 2013; 7(11): 2192–2205. https://doi.org/10.1038/ismej.2013.96 PMID: 23804152

14. Bristow LA, Dalsgaard T, Tiano L, Mills DB, Bertagnolli AD, et al. Ammonium and nitrite oxidation at nanomolar oxygen concentrations in oxygen minimum zone waters. Proc Nat Acad Sci, 2016; 113(38): 10601–6. https://doi.org/10.1073/pnas.1600359113 PMID: 27601665

15. Thamdrup B, Dalsgaard T, Revsbech NP. Widespread functional anoxia in the oxygen minimum zone of the Eastern South Pacific. Deep Sea Res Part I: Oceanogr Res Papers. 2012; 65: 36–45. https://doi.org/10.1016/j.dsr.2012.03.001

16. Tiano L, Garcia-Robledo E, Dalsgaard T, Devol AH, Ward BB, Ulloa O, et al. Oxygen distribution and aerobic respiration in the north and south eastern tropical Pacific oxygen minimum zones. Deep Sea Research Part I: Oceanograph Res Papers. 2014; 94: 173–83. https://doi.org/10.1016/j.dsr.2014.10.001

17. Dalsgaard T, Stewart FJ, Thamdrup B, De Brabandere L, Revsbech NP, Ulloa O, et al. Oxygen at nanomolar levels reversibly suppresses process rates and gene expression in anammox and denitrification in the oxygen minimum zone off northern Chile. MBio. 2014; 5(6): e01966–14. https://doi.org/10.1128/mBio.01966-14 PMID: 25352619

18. Lam P, Lavik G, Jensen MM, van de Vossenberg J, Schmid M, Woebken D, Gutiérrez D, et al. Revising the nitrogen cycle in the Peruvian oxygen minimum zone. Proc Nat Acad Sci. 2009; 106(12): 4752–4757. https://doi.org/10.1073/pnas.0812444106 PMID: 19255441

19. Lam P, Kuypers MM. Microbial nitrogen cycling processes in oxygen minimum zones. Ann Rev Mar Sci. 2011; 3: 317–345. https://doi.org/10.1146/annurev-marine-120709-142814 PMID: 21329208

20. Costa E, Pérez J, Kreft JU. Why is metabolic labour divided in nitrification? Trends Microbiol. 2006; 14 (5): 213–219. https://doi.org/10.1016/j.tim.2006.03.006 PMID: 16621570

21. Gruber N. The marine nitrogen cycle: overview and challenges. In: Capone D.G, Bronk D.A., Mulholland M.R., and Carpenter E.Jeditors. Nitrogen in the marine environment, 2nd ed. Amsterdam: Elsevier. 2008; p. 1–50.

22. Ward BB. Nitrification in marine systems. In: Capone DG, Bronk DA, Mulholland MR, Carpenter EJ, editors. Nitrogen in the marine environment. 2nd ed. Cambridge, MA: Academic Press. 2008; Chapter 5, pp. 199–261.

23. Mashifane TB, Vichi M, Waldron HN, Machu E, Garcon V. Modelling nitrite dynamics and associated feedback processes in the Benguela oxygen minimum zone. Cont Shelf Res. 2016; 124: 200–212. https://doi.org/10.1016/j.csr.2016.05.004

24. Fennel W. Theory of the Benguela upwelling system. J Phys Oceanograph. 1999; 29(2):177–90. https://doi.org/10.1175/1520-0485(1999)029<0177:TOTBUS>2.0.CO;2

25. Carr ME. Estimation of potential productivity in Eastern Boundary Currents using remote sensing. Deep Sea Res Part II: Topical Studies Oceanograph. 2001; 49(1–3): 59–80. https://doi.org/10.1016/S0967-0645(01)00094-7

26. Ulloa O, Canfield DE, DeLong EF, Letelier RM, Stewart FJ. Microbial oceanography of anoxic oxygen minimum zones. Proc Nat Acad Sci. 2012; 109(40): 15996–16003. https://doi.org/10.1073/pnas.1205009109 PMID: 22967509

27. Capone DG, Hutchins DA. Microbial biogeochemistry of coastal upwelling regimes in a changing ocean. Nature Geosci. 2013; 6(9): 711–717. https://doi.org/10.1038/ngeo1916

28. Karstensen J, Stramma L, Visbeck M. Oxygen minimum zones in the eastern tropical Atlantic and Pacific oceans. Prog Oceanogr. 2008; 77(4): 331–350. https://doi.org/10.1016/j.pocean.2007.05.009

29. Kuypers MM, Lavik G, Woebken D, Schmid M, Fuchs BM, Amann R, et al. Massive nitrogen loss from the Benguela upwelling system through anaerobic ammonium oxidation. Proc Nat Acad Sci. 2005; 102 (18): 6478–6483. https://doi.org/10.1073/pnas.0502088102 PMID: 15843458

30. Frame CH, Deal E, Nevison CD, Casciotti KL. N_2O production in the eastern South Atlantic: Analysis of N_2O stable isotopic and concentration data. Global Biogeochem Cycles. 2014; 28(11): 1262–1278. https://doi.org/10.1002/2013GB004790

31. Stramma L, Johnson GC, Sprintall J, Mohrholz V. Expanding oxygen-minimum zones in the tropical oceans. Science. 2008; 320(5876): 655–658. https://doi.org/10.1126/science.1153847 PMID: 18451300

32. Codispoti LA, Friederich GE, Packard TT, Glover HE, Kelly PJ, Spinrad RW, Barber RT, Elkins JW, Ward BB, Lipschultz F, Lostaunau N. High nitrite levels off northern Peru: A signal of instability in the marine denitrification rate. Science. 1986; 233(4769): 1200–2. https://doi.org/10.1126/science.233.4769.1200 PMID: 17756872

33. Herfort L, Schouten S, Abbas B, Veldhuis MJ, Coolen MJ, Wuchter C, et al. Variations in spatial and temporal distribution of Archaea in the North Sea in relation to environmental variables. FEMS Microbiol Ecol. 2007; 62(3): 242–257. https://doi.org/10.1111/j.1574-6941.2007.00397.x PMID: 17991018

34. Cao H, Auguet JC, Gu JD. Global ecological pattern of ammonia-oxidizing archaea. PLoS One. 2013; 8(2): e52853. https://doi.org/10.1371/journal.pone.0052853 PMID: 23468838

35. Peng X, Fuchsman CA, Jayakumar A, Warner MJ, Devol AH, Ward BB. Revisiting nitrification in the Eastern Tropical South Pacific: a focus on controls. Geophys Res Oceans. 2016; 121(3): 1667–1684. https://doi.org/10.1002/2015JC011455

36. Peng X, Jayakumar A, Ward BB. Community composition of ammonia-oxidizing archaea from surface and anoxic depths of oceanic oxygen minimum zones. Front Microbiol. 2013; 4: 177. https://doi.org/10.3389/fmicb.2013.00177 PMID: 23847601

37. Mincer TJ, Church MJ, Taylor LT, Preston C, Karl DM, DeLong EF. Quantitative distribution of presumptive archaeal and bacterial nitrifiers in Monterey Bay and the North Pacific Subtropical Gyre. Environ Microbiol. 2007; 9(5): 1162–1175. https://doi.org/10.1111/j.1462-2920.2007.01239.x PMID: 17472632

38. Tolar BB,. King GM, Hollibaugh JT. An analysis of thaumarchaeota populations from the northern gulf of Mexico. Front Microbiol. 2013; 4: 72. https://doi.org/10.3389/fmicb.2013.00072 PMID: 23577005

39. Mengis M, Gächter R, Wehrli B. Sources and sinks of nitrous oxide (N_2O) in deep lakes. Biogeochem. 1997; 38(3): 281–301. https://doi.org/10.1023/A:1005814020322

40. McIlvin MR, Casciotti KL. Fully automated system for stable isotopic analyses of dissolved nitrous oxide at natural abundance levels. Limnol Oceanogr Methods. 2010; 8(2): 54–66. https://doi.org/10.4319/lom.2010.8.54

41. Frame CH, Lau E, Nolan EJ, Goepfert TJ, Lehmann MF. Acidification enhances hybrid nitrous oxide (N_2O) production associated with aquatic ammonia-oxidizing microorganisms. Front Microbiol. 2017, 7: 2104. https://doi.org/10.3389/fmicb.2016.02104 PMID: 28119667

42. Weiss RF, Price BA Nitrous oxide solubility in water and seawater. Mar Chem. 1980; 8(4): 347–359. https://doi.org/10.1016/0304-4203(80)90024-9

43. McIlvin MR, Altabet MA. Chemical conversion of nitrate and nitrite to nitrous oxide for nitrogen and oxygen isotopic analysis in freshwater and seawater. Anal Chem. 2005; 77(17): 5589–95. https://doi.org/10.1021/ac050528s PMID: 16131070

44. Caporaso JG, Kuczynski J, Stombaugh J, Bittinger K, Bushman FD, Costello EK, et al. QIIME allows analysis of high-throughput community sequencing data. Nature Methods. 2010; 7(5): 335–336. https://doi.org/10.1038/nmeth.f.303 PMID: 20383131

45. Kozich JJ, Westcott SL, Baxter NT, Highlander SK, Schloss PD. Development of a dual-index sequencing strategy and curation pipeline for analyzing amplicon sequence data on the MiSeq Illumina sequencing platform. Appl Environ Microbiol. 2013; 79(17): pp. 5112–5120. https://doi.org/10.1128/AEM.01043-13 PMID: 23793624

46. Caporaso JG, Lauber CL, Walters WA, Berg-Lyons D, Huntley J, Fierer N, et al. Ultra-high-throughput microbial community analysis on the Illumina HiSeq and MiSeq platforms. ISME J. 2012; 6(8): 1621–1624. https://doi.org/10.1038/ismej.2012.8 PMID: 22402401

47. Masella AP, Bartram AK, Truszkowski JM, Brown DG, Neufeld JD. PANDAseq: paired-end assembler for illumina sequences. BMC bioinformatics. 2012; 13(1): 31. https://doi.org/10.1186/1471-2105-13-31 PMID: 22333067

48. Lynch MD, Masella AP, Hall MW, Bartram AK, Neufeld JD. AXIOME: automated exploration of microbial diversity. GigaSci. 2013; 2(1): 3. https://doi.org/10.1186/2047-217X-2-3 PMID: 23587322

49. Altschul SF, Gish W, Miller W, Myers EW, Lipman DJ. Basic local alignment search tool. J Mol Biol. 1990; 215: 403–410. https://doi.org/10.1016/S0022-2836(05)80360-2 PMID: 2231712

50. Edgar RC. Search and clustering orders of magnitude faster than BLAST. Bioinformatics. 2010; 26 (19): 2460–2461. https://doi.org/10.1093/bioinformatics/btq461 PMID: 20709691

51. Edgar RC, Haas BJ, Clemente JC, Quince C, Knight R. UCHIME improves sensitivity and speed of chimera detection. Bioinformatics. 2011; 27(16): 2194–2200. https://doi.org/10.1093/bioinformatics/btr381 PMID: 21700674

52. Cole JR, Wang Q, Cardenas E, Fish J, Chai B, Farris RJ, et al. The Ribosomal Database Project: improved alignments and new tools for rRNA analysis. Nuc Acids Res. 2009; 37(suppl 1): D141–D145. https://doi.org/10.1093/nar/gkn879 PMID: 19004872

53. DeSantis TZ, Hugenholtz P, Larsen N, Rojas M, Brodie EL, Keller K, et al. Greengenes, a chimera-checked 16S rRNA gene database and workbench compatible with ARB. Appl Environ Microbiol. 2006; 72(7): 5069–5072. https://doi.org/10.1128/AEM.03006-05 PMID: 16820507

54. Kumar S, Stecher G, Tamura K. MEGA7: Molecular Evolutionary Genetics Analysis version 7.0 for bigger datasets. Mol Biol Evol. 2016; 33(7): 1870–4. https://doi.org/10.1093/molbev/msw054 PMID: 27004904

55. Benson DA, Cavanaugh M, Clark K, Karsch-Mizrachi I, Lipman DJ, Ostell J, et al. GenBank. Nucleic Acids Res. 2017; 45(D1):D37–42. https://doi.org/10.1093/nar/gkw1070 PMID: 27899564

56. Oksanen F, Blanchet G, Friendly M, Kindt R, Legendre P, McGlinn D, et al. (2017). Package 'vegan.' Community Ecology Package. R package version 2.4–3. 2017; 2(9). Available from: https://CRAN.R-project.org/package=vegan

57. Lau E, Nolan IV EJ, Dillard ZW, Dague RD, Semple AL, Wentzell WL. High throughput sequencing to detect differences in methanotrophic Methylococcaceae and Methylocystaceae in surface peat, forest soil, and *Sphagnum* moss in cranesville swamp preserve, West Virginia, USA. Microorganisms. 2015; 3: 113–136. https://doi.org/10.3390/microorganisms3020113 PMID: 27682082

58. Kindt R, Coe R. Tree diversity analysis. A manual and software for common statistical methods for ecological and biodiversity studies. World Agroforestry Centre (ICRAF), Nairobi. 2005. p. 196.

59. Wickham H. ggplot2: Elegant Graphics for Data Analysis. New York: Springer-Verlag. 2016.

60. de Vries A, Ripley BD. ggdendro: Create Dendrograms and Tree Diagrams Using'ggplot2'. R package version 0.1–20. Available from: http://CRAN.Rproject.org/package=ggdendro. 2016.

61. Santoro AE, Dupont CL, Richter RA, Craig MT, Carini P, McIlvin MR, et al. Genomic and proteomic characterization of "*Candidatus* Nitrosopelagicus brevis": an ammonia-oxidizing archaeon from the open ocean. Proc Nat Acad Sci. 2015; 112(4): 1173–1178. https://doi.org/10.1073/pnas.1416223112 PMID: 25587132

62. Bayer B, Vojvoda J, Offre P, Alves RJ, Elisabeth NH, Garcia JA, et al. Physiological and genomic characterization of two novel marine thaumarchaeal strains indicates niche differentiation. ISME J. 2015; 10: 1051–1063. https://doi.org/10.1038/ismej.2015.200 PMID: 26528837

63. Rice MC, Norton JM, Valois F, Bollmann A, Bottomley PJ, Klotz MG, et al. Complete genome of *Nitrosospira briensis* C-128, an ammonia-oxidizing bacterium from agricultural soil. Standards Genom. Sci. 2016; 11(1): 46. https://doi.org/10.1186/s40793-016-0168-4 PMID: 27471578

64. Off S, Alawi M, Spieck E. Enrichment and physiological characterization of a novel *Nitrospira*-like bacterium obtained from a marine sponge. Appl Environ Microbiol. 2010; 76(14): 4640–4646. https://doi.org/10.1128/AEM.00320-10 PMID: 20511427

65. Löscher CR, Kock A, Könneke M, LaRoche J, Bange HW, Schmitz RA. Production of oceanic nitrous oxide by ammonia-oxidizing archaea. Biogeosci. 2012; 9(7): 2419–2429. https://doi.org/10.5194/bg-9-2419-2012

66. Beman JM, Popp BN, Francis CA. Molecular and biogeochemical evidence for ammonia oxidation by marine Crenarchaeota in the Gulf of California. ISME J 2008; 2(4): 429–441. https://doi.org/10.1038/ismej.2007.118 PMID: 18200070

67. Molina V, Belmar L, Ulloa O. High diversity of ammonia-oxidizing archaea in permanent and seasonal oxygen-deficient waters of the eastern South Pacific. Environ Microbiol. 2010; 12(9): 2450–2465. https://doi.org/10.1111/j.1462-2920.2010.02218.x PMID: 20406296

68. Santoro AE, Casciotti KL, Francis CA. Activity, abundance and diversity of nitrifying archaea and bacteria in the central California Current. Environ Microbiol. 2010; 12(7): 1989–2006. https://doi.org/10.1111/j.1462-2920.2010.02205.x PMID: 20345944

69. Bouskill NJ, Eveillard D, Chien D, Jayakumar A, Ward BB. Environmental factors determining ammonia-oxidizing organism distribution and diversity in marine environments. Environ Microbiol. 2012; 14 (3): 714–729. https://doi.org/10.1111/j.1462-2920.2011.02623.x PMID: 22050634

70. Martens-Habbena W, Qin W, Horak RE, Urakawa H, Schauer AJ, Moffett JW, et al. The production of nitric oxide by marine ammonia-oxidizing archaea and inhibition of archaeal ammonia oxidation by a nitric oxide scavenger. Environ Microbiol. 2015; 17(7): 2261–2274. https://doi.org/10.1111/1462-2920.12677 PMID: 25420929

71. Stewart FJ, Ulloa O, DeLong EF. Microbial metatranscriptomics in a permanent marine oxygen minimum zone. Environmental microbiology. 2012; 14(1): 23–40. https://doi.org/10.1111/j.1462-2920.2010.02400.x PMID: 21210935

72. Levipan HA, Molina V, Fernandez C. *Nitrospina*-like bacteria are the main drivers of nitrite oxidation in the seasonal upwelling area of the Eastern South Pacific (Central Chile ~36˚S). Environ Microbiol Rep. 2014; 6(6): 565–573. https://doi.org/10.1111/1758-2229.12158 PMID: 25756109

73. Arévalo-Martínez DL, Steinhoff T, Brandt P, Körtzinger A, Lamont T, Rehder G, Bange HW. N_2O emissions from the northern Benguela upwelling system. Geophys Res Lett. 2019; 46(6), 3317–3326. https://doi.org/10.1029/2018GL081648

74. Zakem EJ, Al-Haj A, Church MJ, Dijken GL, Dutkiewicz S, Foster SQ, Fulweiler RW, Mills MM, Follows MJ. Ecological control of nitrite in the upper ocean. Nature communications. 2018; 9(1): 1206. https://doi.org/10.1038/s41467-018-03553-w PMID: 29572474

75. Lomas MW, Lipschultz F. Forming the primary nitrite maximum: Nitrifiers or phytoplankton? Limnol Oceanogr, 2006; 51(5): 2453–2467. https://doi.org/10.4319/lo.2006.51.5.2453

76. Hanson RS, Hanson TE. Methanotrophic bacteria. Microbiol Rev. 1996; 60(2): 439–471. PMID: 8801441

77. Stahl DA, de la Torre JR. Physiology and diversity of ammonia-oxidizing archaea. Ann Rev Microbiol. 2012; 66: 83–101. https://doi.org/10.1146/annurev-micro-092611-150128 PMID: 22994489

78. Daebeler A, Bodelier PL, Yan Z, Hefting MM, Jia Z, Laanbroek HJ. Interactions between Thaumarchaea, *Nitrospira* and methanotrophs modulate autotrophic nitrification in volcanic grassland soil. ISME J. 2014; 8(12), 2397–2410. https://doi.org/10.1038/ismej.2014.81 PMID: 24858784

79. Babbin AR, Keil RG, Devol AH, Ward BB. Organic matter stoichiometry, flux, and oxygen control nitrogen loss in the ocean. Science, 2014; 344: 406–408. https://doi.org/10.1126/science.1248364 PMID: 24763588

80. Schmid MC, Risgaard-Petersen N, Van De Vossenberg J, Kuypers MM, Lavik G, Petersen J, et al. Anaerobic ammonium-oxidizing bacteria in marine environments: widespread occurrence but low diversity. Environ Microbiol. 2007; 9(6): 1476–1484. https://doi.org/10.1111/j.1462-2920.2007.01266.x PMID: 17504485

81. Klindworth A, Pruesse E, Schweer T, Peplies J, Quast C, Horn M, et al. Evaluation of general 16S ribosomal RNA gene PCR primers for classical and next-generation sequencing-based diversity studies. Nuc Acids Res. 2013; 41(1): e1. https://doi.org/10.1093/nar/gks808 PMID: 22933715

82. Beman JM, Carolan, MT. Deoxygenation alters bacterial diversity and community composition in the ocean's largest oxygen minimum zone. Nature Comm. 2013; 4: 2705. https://doi.org/10.1038/ncomms3705 (2013) PMID: 24162368

83. Bryant JA, Stewart FJ, Eppley JM, DeLong EF. Microbial community phylogenetic and trait diversity declines with depth in a marine oxygen minimum zone. Ecology. 2012; 93(7): 1659–1673. https://doi.org/10.1890/11-1204.1 PMID: 22919912

84. Gruber N, Sarmiento, JL. Global patterns of marine nitrogen fixation and denitrification. Global Biogeochem Cycles. 1997; 11(2): 235–266.

85. Codispoti LA, Brandes JA, Christensen JP, Devol AH, Naqvi SWA, Paerl HW, et al. The oceanic fixed nitrogen and nitrous oxide budgets: Moving targets as we enter the anthropocene? Scientia Marina, 2001; 65(S2): 85–10. https://doi.org/10.3989/scimar.2001.65s285

86. Schmidtko S, Stramma L, Visbeck M. Decline in global oceanic oxygen content during the past five decades. Nature. 2017; 542(7641): 335–339. https://doi.org/10.1038/nature21399 PMID: 28202958

87. Philips S, Laanbroek HJ, Verstraete W. Origin, causes and effects of increased nitrite concentrations in aquatic environments. Rev Environ Sci Biotech. 2002; 1(2): 115–141. https://doi.org/10.1023/A:1020892826575

88. Stein LY, Arp DJ. Loss of ammonia monooxygenase activity in *Nitrosomonas europaea* upon exposure to nitrite. Appl Environ Microbiol. 1998; 64(10): 4098–4102. PMID: 9758853

89. Beaumont HJ, Hommes NG, Sayavedra-Soto LA, Arp DJ, Arciero DM, Hooper AB, et al. Nitrite reductase of *Nitrosomonas europaea* is not essential for production of gaseous nitrogen oxides and confers tolerance to nitrite. J Bacteriol. 2002; 184(9): 2557–2560. https://doi.org/10.1128/JB.184.9.2557-2560.2002 PMID: 11948173

90. Arp DJ, Stein LY. Metabolism of inorganic N compounds by ammonia-oxidizing bacteria. Crit Rev Biochem Mol Biol. 2003; 38(6): 471–495. https://doi.org/10.1080/10409230390267446 PMID: 14695127